

THE PHYSICAL AND CHEMICAL DEGRADATION OF PWR FUEL RODS IN SEVERE ACCIDENT CONDITIONS

P.D. PARSONS, J.A.S. MOWAT, D.W.F. DEWHURST
UKAEA Northern Division,
Springfields Nuclear Power Development Laboratories,
Springfields, Salwick

T.E. HUGHES
British Nuclear Fuels Limited,
Springfields, Salwick

United Kingdom

ABSTRACT

An experimental study of the interaction between Zircaloy-4 cladding and UO_2 in PWR fuel rods heated to high temperatures with a negligible differential pressure across the cladding wall is described. The fuel rods were of dimensions appropriate to the 17 x 17 PWR fuel sub-assembly and were heated in a non-oxidising environment (vacuum) up to $\sim 1850^\circ C$ either isothermally or through heating ramps. Observations were made concerning the extent and nature of the reaction zone between Zircaloy-4 and UO_2 over the temperature range 1500-1850 $^\circ C$ for times ranging from 1 min to 125 min. The location, morphology and the chemical composition of the phases formed are described along with the kinetics of their formation.

INTRODUCTION

The probability of a severe accident in a LWR, that is an accident in which the core is degraded, is exceedingly remote. Nevertheless, it is important to understand the way in which fuel and core components would behave in such an accident. The initial heating of the fuel, after loss of coolant and reactor shut down, arises from the decay heat. As the temperature rises, given the availability of steam, additional heat will be generated by the exothermic Zircaloy-steam reaction. If cooling is not re-established, eventually the temperature of the fuel will rise until liquid phases are formed either by eutectic liquation or simply by melting.

As yet there is no accepted quantitative model of core heat-up although work is currently in progress^(1,2). Chung⁽³⁾ has also considered the materials reactions that may occur during the heating of fuel up to and beyond temperatures at which Zircaloy melts. The first liquid phase formed depends on the contact between cladding and fuel. With contact, a low melting Zr-U-O eutectic forms in the cladding but without contact Zircaloy melts on the inner diameter of the cladding at $\sim 1900^\circ C$. Molten Zircaloy dissolves UO_2 and 'candles' down the fuel rod. The formation of

liquid phases is important since they are mobile and may relocate and freeze in the fuel assembly sub-channels inhibiting subsequent cooling of the damaged fuel. Apart from reactions between fuel and cladding there is potential for reactions between other core components such as grids, control rods and absorber materials.

The work reported in this paper describes the initial part of a programme of work at Springfields Nuclear Power Development Laboratories, designed to investigate the degradation of PWR fuel in conditions leading to severe fuel damage. The work performed in this preliminary part of the programme has been to study the reaction between Zircaloy-4 and UO_2 heated in contact, in an inert environment, i.e. vacuum, to a temperature of $\sim 1850^\circ C$.

Zircaloy is oxidised by UO_2 when in contact at high temperature⁽⁴⁾ and the extent of the oxidation and the redistribution of material involved in the reaction may influence the subsequent progression of fuel damage. Measurements of the extent of reaction between Zircaloy-4 and UO_2 and observations on the nature of the chemical redistribution involved have been made over the temperature range 1500-1800 $^\circ C$ for times ranging from 1 to 125 min. The reactions are described in terms of the sequence and composition of the phases formed and the kinetics of their formation.

EXPERIMENTAL METHODS

Short fuel rods, between 150 and 300 mm in length, were made using Zircaloy-4 tubing of 9.5 mm outer diameter and 0.57 mm wall thickness loaded with 13 mm long UO_2 fuel pellets of 95% theoretical density.

The UO_2 pellets were ground to a diameter to give a sliding fit in the Zircaloy tubing. The typical Zircaloy cladding inner diameter was 8.36 ± 0.004 mm. The differential expansion on heating to high temperatures ensured good contact between the UO_2 pellet and cladding. Calculations of the thermal expansion of the pellet and the cladding using thermal expansion data in MATPRO⁽⁵⁾ show that with initial diameters in the ranges quoted above, good contact should occur at temperatures above $\sim 1000^\circ C$ providing the temperature of the pellet does not lag significantly behind that of the cladding.

End caps were welded under argon on both ends of the fuel rod, one end cap having a hole (dia. 0.8 mm) to allow equalisation of the pressure in the fuel rod with that of the vacuum chamber.

The fuel rods were heated in a 80 mm dia. 1070 mm long Vitreosil tube maintained under dynamic vacuum. The construction of the apparatus is shown schematically in Fig. 1. The fuel rods were heated by radiation from a concentric surrounding graphite susceptor ~ 70 mm long, 20 mm inner dia. and 1 mm wall thickness. The graphite susceptor was heated by induction from a water cooled copper coil wound externally on the Vitreosil tube and energised from a 6 kW, 450 kHz induction generator. The top of the reaction vessel was sealed using an O-ring and flange and housed a quartz window for sighting the fuel rod with a pyrometer. The lower end of the reaction vessel was connected to a conventional dynamic vacuum system.

The temperature of the fuel rod was measured using a disappearing filament pyrometer calibrated using a W/W-26% Re thermocouple attached to the centre of a fuel rod and agreement at 1500°C was within 10°C.

Some fuel rods were heated rapidly and held at isothermal temperatures of 1500, 1650 and 1800°C for times ranging from 5 to 125 min at 1500°C and 1 to 50 min at 1650 and 1800°C. Some fuel rods were heated to maximum temperature at various heating rates, the maximum heating rate and maximum temperature achieved was 4 °C s⁻¹ up to 1600°C and 2.7 °C s⁻¹ from 1600-1850°C.

RESULTS

After heating, all the rods were intact although brittle, and some broke easily on handling. Rods heated for short times or at 1650°C were bright and exhibited metal spalling. Rods heated for longer times at 1800°C showed evidence of surface melting at the central location. Figure 2 shows the appearance of rods heated isothermally and through temperature ramps.

MICROSTRUCTURES OF THE REACTED ZONES

Sections were cut from the centre of heated rods for optical microscopy, electron probe microanalysis and Auger electron microscopy. Optical sections were polished and etched either by attack polish in HF and Cr₂O₃ or by swab etching in 55% lactic acid, 19% nitric acid, 19% water and 7% HF.

The location of phases formed and their morphology were determined by optical microscopy. The microstructures of rods heated isothermally at 1500, 1650 and 1800°C exhibit a similar characteristic distribution of phases which becomes increasingly complex as the time and temperature increase. The major phases formed consist of concentric bands of material similar to those described by Hoffman and co-workers^(4,6) after heating fuel rods in argon under pressure to temperatures between 1000 and 1700°C.

The Zircaloy is oxidised by the UO₂ and the increased oxygen concentration in Zircaloy results in the formation of the high oxygen-stabilised α-Zr[O] phase. The extent to which this phase grows radially across the cladding depends upon the extent of oxygen diffusion from the UO₂ fuel pellet. Simultaneously, uranium diffuses outwards from the fuel pellet to form a uranium rich phase in the Zircaloy cladding. Additionally some zirconium diffuses inwards from the original Zircaloy-UO₂ boundary to form α-Zr[O]. The general distribution of phases is shown in Fig. 3. From the UO₂-Zircaloy boundary, each phase layer is referred to as layer I, layer II etc. as illustrated in Fig. 3 and previously described by Hoffman and Politis⁽⁴⁾. The oxygen stabilised alpha-Zircaloy phase nearest the UO₂ fuel pellet is referred to as α-Zr[O]a, and that nearer the cladding outer diameter as α-Zr[O]b.

Isothermally heated fuel rods

Figure 4 illustrates the typical microstructures of fuel rods heated for 25 min at 1500, 1650 and 1800°C. The outer boundary of the U/Zr phase (layer II) is only smooth at 1500°C and for times ≤ 25 min. At higher temperatures and longer times the boundary becomes increasingly irregular (see Fig. 4(b) and (c)) and eventually the U/Zr phase becomes almost totally dispersed in the Zircaloy as illustrated in Fig. 4(d). After 5 min at 1500°C the α-Zr[O]b phase has moved to just beyond the mid-plane of the cladding wall. After 25 min at 1500°C the α-Zr[O]b phase has grown almost to the cladding outer diameter. At 1650°C, after 25 min, the U/Zr phase (layer II) is evident more as a globular phase than a band of material. At 1800°C, even for times as short as 1 min, the outer boundary of the U/Zr phase is always very irregular and highly structured exhibiting an acicular morphology and at times > 5 min the U/Zr phase has a globular appearance.

The macrographs of the fuel pellet and cladding cross sections in Fig. 4 illustrate the progressive development of voids, first at the UO₂/cladding interface and subsequently within the cladding wall thickness. Radiography of the intact post-test fuel rods also clearly revealed voids in the cladding wall eliminating the possibility that apparent voids resulted from polishing artefacts. The void volume increases with time at isothermal temperature and with temperature at constant time. The voids were located consistently on the UO₂/layer I and the layer I/layer II boundaries, apart from the fuel rod heated at 1500°C for 5 min which had voids in the layer I phase but not at the UO₂/layer I boundary. The voids at the UO₂/layer I boundary generally remained small whereas the voids at the layer I/layer II boundary grew relatively large.

Scanning electron microscopy of transverse fracture surfaces of reacted cladding clearly revealed voids, shown in Fig. 5. The void surfaces were smooth and rounded suggesting the presence of a once molten surface.

In all the isothermally heated fuel rods, small particles of a metallic phase (later shown to be uranium) were observed and in fuel rods heated longer than 25 min at 1650°C or higher temperatures, a region of mottled contrast was sometimes observed within the apparent UO₂/cladding boundary. The phases present in this region were analysed by EPMA.

Ramp heated fuel rods

Fuel rods were ramp heated at a range of heating rates varying from ~ 4 °C s⁻¹ to 1850°C, i.e. taking ~ 4 min to reach 1850°C from 1000°C to the slower heating rate of ~ 0.5 °C s⁻¹ taking 23 min to rise from ~ 800°C to ~ 1500°C. Ramp heated rods were sectioned for optical microscopy longitudinally and Fig. 6 shows the penetration of the inter-pellet gaps, presumably by once liquid material drawn in by capillary action in a fuel rod ramp heated to ~ 1850°C at ~ 4 °C s⁻¹. Melting of the cladding is apparent from the thickening of the cladding at the lower end of the rod.

The microstructure of the once molten region is complex, resembling a eutectic structure, and varies across the thickness of the cladding. The apparent volume fraction of voids is much greater in the central region of the rod, where peak temperature occurs, but voids are still present in the upper and lower region and also in the thickened region overlaid with once molten material.

KINETICS OF THE UO₂-ZIRCALOY-4 REACTION

The movements of the concentric phase boundaries are functions of time and temperature and are related to the flux of oxygen into the Zircaloy as a result of the oxidation of the cladding by the UO₂ fuel.

The temperature and time dependencies of the rate of boundary movement have been determined by measuring the position of the concentric phase boundaries using optical microscopy. The diameters of the UO₂/cladding, the α -Zr[O]a (layer I) and the U/Zr (layer II) boundaries were measured at far orthogonal locations. The dimensions of the layers I, II and III were obtained by difference and are listed in Table 1. The gross unevenness of the layer II boundary and the presence of many voids results in a large scatter for the measurement of the position of the layer II boundary which eventually broke up as the U/Zr phase became widely dispersed. The variation of the distance of a boundary from the centre of the fuel pellet (measured diameter \times 0.5) as a function of time and temperature is shown in Fig. 7. The boundary between the UO₂ phase and the cladding moves inwards from the initial pellet/cladding boundary to a nearly constant position irrespective of the temperature between 1500-1800°C. The outer boundary of α -Zr[O]a (layer I) moved outwards and the relative position of the original UO₂ pellet/cladding boundary, i.e. within the α -Zr[O]a (layer I) phase, was confirmed by heating fuel rods containing inert tungsten marker wires between the UO₂ pellet and cladding. Good initial contact between the cladding and UO₂ either side of the marker wire was ensured by externally pressurising the fuel rod before testing. This was achieved in an autoclave under argon at 900°C and 12 MPa. The position of the marker wire in a fuel rod heated for 15 min at 1650°C is shown in Fig. 8 and the original UO₂/cladding boundary is about one-third of the α -Zr[O]a thickness away from the reacted UO₂/cladding boundary.

The distances from the fuel pellet boundary and the width of the α -Zr[O]a (layer I) and U/Zr (layer II) phases are listed in Table 1 as a function of time for the temperatures 1500, 1650 and 1800°C and are plotted against \sqrt{t} in Fig. 9. In only two fuel rods, those heated at 1500°C for 5 min and 1650°C for 1 min, the α -Zr[O]b layer did not advance to the outer diameter, the position of the α -Zr[O]b (layer II) boundary for these two fuel rods is also plotted in Fig. 9 but is regarded as approximate. The advance of the layer I and layer II outer boundaries initially obey a parabolic rate law and the assumption has been made that the parabolic rate is temperature dependent according to the Arrhenius relationship. The initial parabolic reaction rates are listed in Table 2 and plotted as a function of 1/T K in Fig. 10.

ELECTRON MICROPROBE ANALYSIS OF PHASES IN REACTED CLADDING

Sections from four fuel rods heated isothermally and one ramp heated fuel rod have been examined using electron probe microanalysis to determine the metallic compositions of phases formed in the reaction. Four isothermally heated fuel rods have also been examined in a scanning Auger microprobe analyser and the oxygen concentration profile across the reacted zone measured using Auger electron spectrometry. For calibration purposes, oxygen in Zircaloy standards were made by oxidation of Zircaloy cladding in an autoclave followed by a vacuum heat treatment homogenisation. The uniformity of the oxygen distribution in the homogenised samples was estimated by measuring the microhardness across the cladding wall and in more detail by neutron microbeam analysis⁽⁷⁾. The standards ranged from 4 to 29 atomic % oxygen in Zircaloy and in addition a nominal 66.7 atomic % in ZrO₂. The sequence and composition of the phases as determined by EPMA and SAM in fuel rods heated both isothermally and ramp heated are as follows.

Fuel rods heated isothermally at 1500°C

The sequence of phases observed in fuel rods heated at 1500°C for times of 5 min and 125 min broadly follows the pattern idealised in Fig. 3. The composition of the layer I phase is 87-89% Zr, 5-7% U, \sim 1% Sn and the remainder of oxygen. This phase is predominantly oxygen stabilised α -Zr with some dissolved uranium. There are also grain boundary and intra-granular phases present and are illustrated in Figs 11 and 12, marked A and B in Fig. 12. These phases have similar compositions being 2-3% Zr, 96-97% U and 0.2-1% Sn with traces of iron and chromium. The layer II phase is predominantly a U-Zr metallic phase and contains almost zero oxygen concentration. In the fuel rod heated for 5 min the composition of the layer II phase varies from 20% Zr-80% U on the inner diameter to \sim 34% Zr-66% U on the outer diameter. After 125 min the layer II composition is increased in uranium and is 3% Zr-97% U. In both fuel rods examined after heating at 1500°C, the U/Zr layer II phase contained inhomogeneous regions. Figure 11 shows the acicular morphology in the layer II phase formed in the fuel rod heated for 5 min at 1500°C. The needles have the composition 95% Zr, 3.5% U, 1.5% Sn in a matrix of a higher uranium concentration U-Zr-Sn composition. Figure 12 shows the phases observed in the layer II phase formed in the fuel rod heated for 125 min at 1500°C. The layer II, U/Zr metallic phase has ceased to be a coherent layer and contains two types of particle marked C and D in Fig. 12. The particle marked C is typical of a number of small polygonal particles of composition 52-77% Zr, 1-19% U, 17-34% Sn and \sim 0.2% (Cr + Fe), i.e. relatively rich in Sn. The average composition measured from a number of particles is 66% Zr, 26% Sn, 7% U and 0.2% (Cr + Fe). Larger irregular shaped phases also form within the U/Zr matrix exemplified by the phase marked D in Fig. 12 and these phases have the composition 8-53% Zr, 38-88% U, 4-14% Fe, 2% Cr and 0-0.3% Sn with an average composition 22% Zr, 65% U, 10% Fe, 2% Cr and 0.1% Sn, i.e. relatively rich in the minor alloying elements of Zircaloy-4, iron and chromium. The composition of

small particles determined by EPMA is regarded as approximate owing to the possibility of the excitation beam penetrating the particles and exciting the underlying material. In both fuel rods heated to 1500°C the layer III phase has the composition 92-95% Zr, 1-4% U and 0.4-1.0% Sn with $\sim 3-5.5\%$ O_2 , i.e. essentially oxygen stabilised α -Zr containing less dissolved uranium than in the α -Zr[O] layer I phase.

The oxygen concentration in layer I of the fuel rod heated for 5 min was $\sim 6.1\%$, in layer III the oxygen concentration decreased from $\sim 5.5\%$ to $\sim 3.3\%$ at the cladding outer diameter. In the fuel rod heated for 125 min the oxygen concentration was uniform in layer I and III being $\sim 4.2\%$.

Fuel rods heated isothermally at 1800°C

The sequence of phases in fuel rods heated isothermally at 1800°C showed significant deviation from the idealised banded structure illustrated in Fig. 3. After ~ 1 min at 1800°C the layer II phase is irregularly distributed across the cladding wall and is highly structured as illustrated in Fig. 13. Layer I has the composition 87% Zr, 7.8% U and $\sim 1\%$ Sn with a constant concentration of $\sim 4.1\%$ oxygen. The grain boundary and intragranular precipitates have the composition 98% U, 1% Zr, 1% Sn and $\sim 1\%$ (Fe + Cr). The layer II matrix composition is 24% Zr, 75% U and $\sim 1\%$ Sn with negligible oxygen concentration. The needle shaped phases observed in parts of the layer II phase (see Fig. 13) have a composition which varies from region to region and is 30-35% Zr, 64-70% U and $\sim 1\%$ (Fe + Cr). The material between the needles has the composition 93% Zr, 7% U. The layer III phase is essentially oxygen stabilised α -Zr of composition 94-95% Zr, $\sim 1\%$ U and $\sim 1\%$ Sn with oxygen varying from $\sim 4.1\%$ at the inner diameter to $\sim 3\%$ at the outer diameter.

In the fuel rod heated for 50 min, layer II is distributed as a few globular, uranium rich regions and small particles of U/Zr phase, distributed completely across the cladding wall thickness, see Fig. 14. The matrix phase varies from $\sim 29\%$ Zr, $\sim 67\%$ U and 4.3% oxygen at the inner diameter to $\sim 92\%$ Zr, $< 2\%$ U, $< 2\%$ Sn and $\sim 4.3\%$ oxygen at the outer diameter. The particles of U/Zr range from $\sim 2 \mu\text{m}$ diameter and approximate composition 84% U, 16% Zr at the inner diameter to $\sim 0.2 \mu\text{m}$ diameter and 40% U, 60% Zr at the outer diameter. The oxygen concentration across the cladding wall is constant at $\sim 4.3\%$.

In all fuel rods heated at 1600°C for longer than 25 min or at higher temperature, a reacted zone was occasionally observed within the apparent UO_2 boundary as illustrated in Fig. 14. Within this region uranium metallic particles and particles of a zirconium rich phase were detected in a matrix of UO_2 . The zirconium rich phase has the composition 89% Zr, 9% U, $\sim 2\%$ Sn.

Ramp heated fuel rod

The fuel rod ramp heated to $\sim 1850^\circ\text{C}$ at $\sim 4^\circ\text{C s}^{-1}$ (shown in Fig. 6) has also been examined by EPMA in the region of wall thickening. This region has a needle-like morphology and the compositions of the needle and matrix phases in an area near the outer diameter are 80% Zr, 10% U, 10% Fe and 70% Zr, 25% U, 5% Fe neglecting any oxygen which may be present.

SUMMARY AND DISCUSSION

Zircaloy and UO_2 react at high temperature once contact is made. The sequences of phases formed when UO_2 fuel pellets and Zircaloy cladding in fuel rods are in contact by virtue of the thermal expansion of the UO_2 , i.e. in non-pressurised conditions, over the temperature range 1500-1800°C is similar to those described for reactions under external pressure^(4,6). From the UO_2 boundary outwards the sequence of phases is, an oxygen stabilised α -Zr[O] phase containing some intragranular and intergranular U/Zr phase; a layer of U/Zr phase; followed by a layer of oxygen stabilised α -Zr[O] phase which after sufficient time at temperature extends to the cladding outer surface, i.e. UO_2 ; α -Zr[O] + U/Zr; U/Zr; α -Zr[O]. The relationship of this sequence of phases to those at equilibrium in the Zr-U-O ternary system at high temperature has previously been described by Hoffman and co-workers^(4,6). The oxidation of the Zircaloy and reduction of the UO_2 is effected by the outward diffusion of oxygen and uranium and the inward diffusion of zirconium, as evidenced by the relative positions of the UO_2 /cladding boundary before and after reaction. The measurements of pre- and post-test UO_2 pellet diameter and the position of the tungsten marker, both indicate the original UO_2 /cladding boundary to be in the α -Zr[O] (layer I) phase and that uranium has been transported through part of the α -Zr[O] phase to the U/Zr layer. The presence of U/Zr phase in the grain boundaries of the α -Zr[O] phase indicates that the transport of uranium could be by intergranular diffusion.

The location and the morphology of the U/Zr phase is markedly dependent on time at temperature. As the temperature or time at temperature increases, the outer boundary of the U/Zr phase becomes increasingly irregular until after 50 min at 1800°C the U/Zr phase is almost totally dispersed across the cladding as small particles, i.e. with increasing oxidation of the Zircaloy the morphology of the U/Zr phase becomes unstable in the higher oxygen activity α -Zr[O] and ceases to be a coherent layer. The break-up of the U/Zr phase is more evident in fuel rods in which the oxygen concentration profile in both α -Zr[O] phases becomes uniform. The U/Zr phase has a very low solubility for oxygen and has a relatively low melting point, i.e. 1500-1100°C for alloys with > 50 weight % uranium, decreasing with increasing uranium concentration⁽⁸⁾. The compositions of the U/Zr phases formed in fuel rods heated in the range 1500-1800°C are such that they will be liquid at the test temperature. On cooling, the U/Zr liquid first solidifies to γ -(U, Zr) continuous solid solution and eventually, below $\sim 750^\circ\text{C}$, undergoes a solid state transformation. The composition and morphology of the transformation products will depend to some extent on the cooling rate and Figs 11 and 13 show that the transformation products are in some regions complex, consisting of alternate needle-like regions of:

- (a) high zirconium, low uranium (93-95 Zr, 3.5-7 U), and
- (b) low zirconium, high uranium (35-20 Zr, 64-66 U).

The minor alloying elements of Zircaloy-4 appear to be more soluble in the U/Zr phase and are precipitated on cooling into small polygonal zirconium rich precipitates with a high concentration of tin ($\sim 26\%$) and also elongated uranium rich precipitates containing a high concentration of iron ($\sim 10\%$). Since there is no external pressure on the fuel rods the

U/Zr phase only penetrates the inter-pellet gap to a small extent, presumably due to capillary forces, see Fig. 6. In the fuel rod heated to $\sim 1850^\circ\text{C}$ at a ramp rate of $\sim 4^\circ\text{C s}^{-1}$, some of the UO_2 pellet appears to have been dissolved by Zircaloy and run down the fuel rod. The solidified structure is of needles of a high zirconium concentration phase ($\sim 95\%$ Zr, $\sim 4\%$ U) and needles of a 65% Zr, 17% U, $12\text{--}15\%$ Fe phase.

In all fuel rods examined metallic uranium was observed in the UO_2 fuel pellet but in fuel rods heated at 1650°C for greater than 25 min or at higher temperature some areas of fuel pellet adjacent to the cladding exhibited zirconium rich material between the UO_2 grains. Figure 14 shows this material as dark contrast in an electron image, which in optical contrast appeared bright. The composition is $\sim 89\%$ Zr, 9% U and $\sim 2\%$ Sn. A uranium rich metallic phase is also present, (bright contrast in the electron image) and contains dissolved alloying elements of Zircaloy, i.e. 96% U, $1\frac{1}{2}\%$ Zr, 0.25% Sn and 2.5% Fe. The U rich phase, U(Zr), appears to form in the UO_2 grain boundaries which at temperature may have caused decohesion of the UO_2 , a process accelerated at higher temperatures by the presence of liquid Zircaloy.

The movement of the phase boundaries through the cladding, relative to the UO_2 /cladding boundary, has been shown to be initially parabolic until the cladding no longer behaves as a semi-infinite sink for oxygen diffusing from the UO_2 . The parabolic rates of boundary movement are plotted in Fig. 10 as a function of reciprocal temperature and are compared with the more extensive data set of Dienst et al⁽⁹⁾ determined from reactions of UO_2 and cladding under an external over-pressure. For the movement of $\alpha\text{-Zr[O]a}$ (layer I), apart from some deviation at 1500°C , the present data are in good agreement at the higher temperature of 1650°C and with the extrapolation to 1800°C . The U/Zr (layer II) outer boundary becomes increasingly irregular and eventually disperses with increasing temperature making it difficult to define the layer II boundary movement and the rates quoted are necessarily associated with a large degree of uncertainty. However, the present data shows good agreement with the data of Dienst et al⁽⁹⁾ and show a tendency to higher rates above $\sim 1500^\circ\text{C}$ than extrapolation from lower temperature data would suggest and also a change in apparent activation energy. The present definition of the measurement of the U/Zr (layer II) boundary movement includes the growth of the $\alpha\text{-Zr[O]a}$ phase with the U/Zr growth. The increased rates at higher temperature relative to the $\alpha\text{-Zr[O]a}$ growth suggest the U/Zr phase thickens at a faster rate at higher temperature with an increased apparent activation energy, however more accurate data are required to substantiate this. The similarity in rates of boundary movement in the temperature range $1500\text{--}1800^\circ\text{C}$ for fuel rods reacted both under high and under negligible external pressure indicates very little effect of external pressure on the kinetics of phase boundary movement.

A more obvious effect of external pressure is on the occurrence of voids in the cladding and the extent of redistribution of liquid U/Zr phase in the UO_2 inter-pellet gaps. The volume fraction of voids formed in the fuel rods heated without external pressure grows with time and temperature and is a relatively large volume fraction of the cladding at 1800°C , see Fig. 4(d). The voids form consistently in two locations, at the UO_2 /

cladding boundary, which moves inwards, and the $\alpha\text{-Zr[O]a/U/Zr}$ boundary. The void growth is greatest at the $\alpha\text{-Zr[O]a/U/Zr}$ boundary where the liquid U/Zr forms. Voids were also observed in zirconium/ UO_2 reactions at $\sim 870^\circ\text{C}$ for long times but not at 1100°C ⁽¹⁰⁾. There is a reduction in volume associated with the formation of the product phases^(10,11), and preliminary calculations of the product volume in the fuel rod heated for 5 min at 1500°C indicate that this is responsible for most of the void formation.

The oxidation of cladding by UO_2 , when in contact at high temperature, increases the susceptibility of the cladding to embrittlement and subsequent fracture by the stresses generated by differential thermal contraction when the fuel is eventually cooled. In LWR accident situations the cladding would be oxidised both on the inner and outer surfaces and the courses of both reactions would be mutually affected.

The present work is currently being extended to oxidise cladding simultaneously by steam on the outer surface and by UO_2 on the inner surface. The resultant reactions up to temperatures of $\sim 1850^\circ\text{C}$ will be characterised.

ACKNOWLEDGEMENT

The authors are indebted to Mr B Riley for the SAM oxygen analyses.

REFERENCES

1. BOWERS C H et al. Status of major modelling phenomena in the ANL/NSAC core heat-up and redistribution (ANCHOR) code. ANL. Argonne, Illinois.
2. ALLISON C M et al. Severe Core Damage Analysis Package (SCDAP) code conceptual design report, EGG-CDAP-5397, April 1981.
3. CHUNG H M. Materials interaction accompanying degraded core accidents. Presented to Faculty Institute on LWR Safety-Degraded Core Cooling Division of Educational Programs, ANL, March 1981.
4. HOFMANN P and POLITIS C. The kinetics of the uranium dioxide-Zircaloy reactions at high temperatures. JNL NUC MATER 98 (1979) p375.
5. MATPRO Version 11 (Revision 1). A handbook of materials properties used in the analysis of LWR fuel rod behaviour. NUREG/CR-0497, February 1980.
6. HOFMANN P and KERWIN D K. Preliminary results of UO_2 /Zircaloy-4 experiments under severe fuel damage conditions. Res Mechanica 5 (1982) 293-308.
7. MCMILLAN J W and PUMMERY F C W. Nuclear microprobe methods for the investigation of the corrosion of Zr-2 and an Fe-44 Ni-17 Cr alloy (PE16). CORROSION SCIENCE 20 (1980) p41-52.

8. ROUGH A F and BAUER A A. BMI-1300, June 1958.
9. DIENST W, HOFMANN P and KERWIN-PECK D. Chemical interactions between UO_2 and Zr-4 in the temperature range 1000-2000°C. KfK-PNS JAHRESKOLLOQUIUM, 1982.
10. MALLET M W et al. BMI-1210, June 1957.
11. PARSONS P D et al. UO_2 -Zircaloy-4 reactions at temperatures up to $\sim 1850^\circ\text{C}$. Unpublished work. March 1983.

TABLE 1

Dimensions of layered phases

Specimen	Temp. °C	Time min	Semi-Diameter of original pellet (specification)	Fuel pellet radius (mm)	Width of layer I $\alpha\text{-ZrO}(a)$ (μm)	Mean radius of layer I/II boundary (mm)	Distance of layer II outer boundary from fuel pellet (μm)	Mean radius of layer II/III boundary (mm)	Distance of layer III outer boundary from fuel pellet (μm)
9	1500	5	4.159-4.153	4.14	55	4.195	130	4.275	180
15	1500	25	"	4.09	135	4.225	210	4.30	-
17	1500	125	"	4.05	260	4.31	330	4.41	-
14	1650	1	"	4.13	80	4.21	260	4.39	300
7	"	5	"	4.06	235	4.295	490	4.54	-
10	"	25	"	4.03	350	4.385	600	4.56	-
16	"	50	"	4.04	390	4.43	555	4.595	-
19	1800	1	"	4.09	155	4.245	350	4.44	-
6	"	5	"	4.07	295	4.355	510	4.57	-
8	"	25	"	4.03	370	-	-	-	-
11	"	50	"	4.04	600	-	-	-	-

TABLE 2

Parabolic rates of reaction for phase boundary movements

		Reaction rate $(\delta)^2/t$ $\text{cm}^2 \text{s}^{-1}$		
		1500°C	1650°C	1800°C
Reaction rate layer I, II, etc.	I	1.27×10^{-7}	1.1×10^{-6}	2.7×10^{-6}
	II	3.4×10^{-7}	8.8×10^{-6}	1.2×10^{-5}

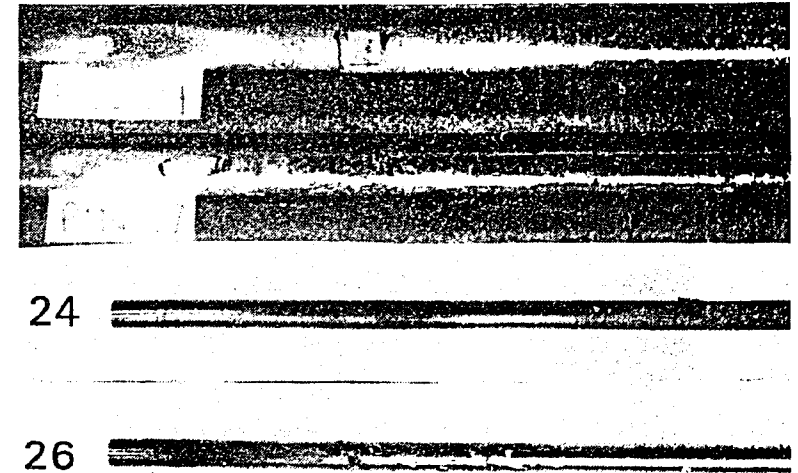
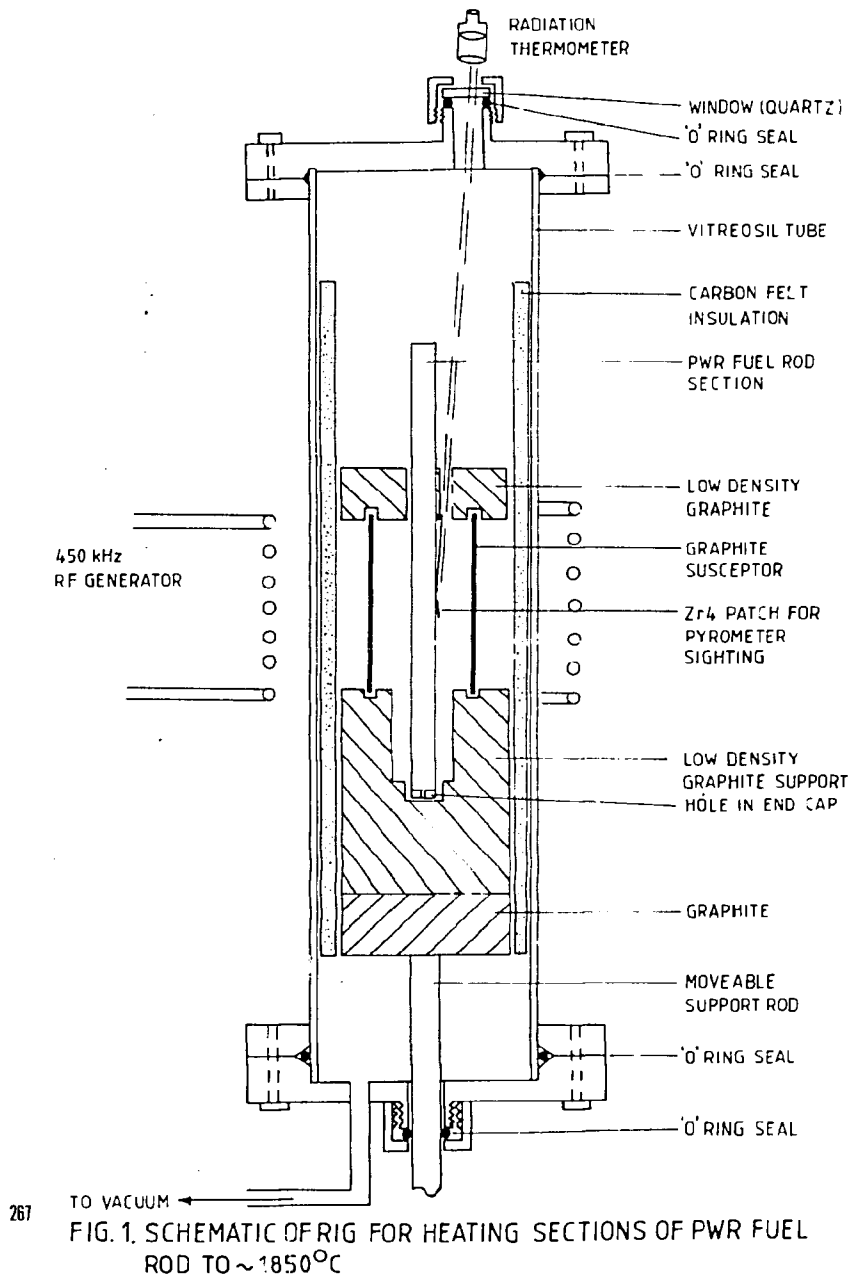


FIG. 2 FUEL RODS HEATED IN A VACUUM. PIN 19 1 MIN AT 1800°C . PIN 17, 125 MIN AT 1500°C . PIN 24 AT 0.5 k s^{-1} TO 1800°C . PIN 26 AT $\sim 4 \text{ k s}^{-1}$ TO $\sim 1850^{\circ}\text{C}$.

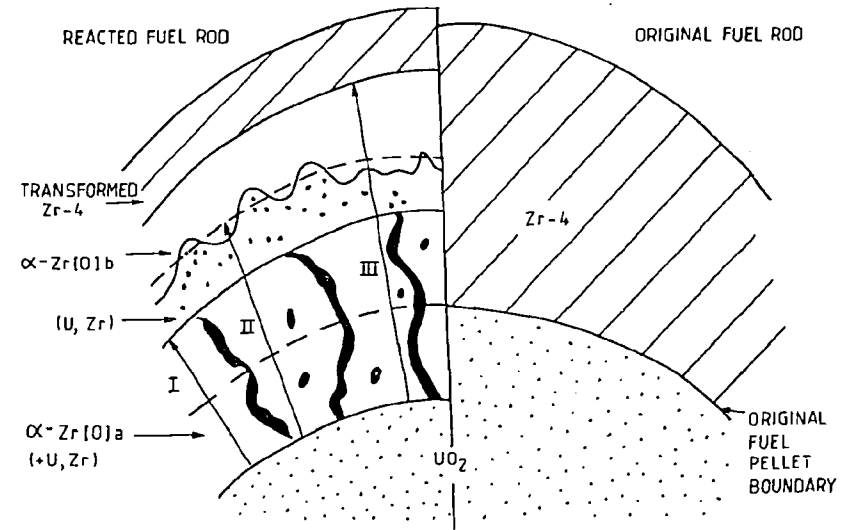


FIG. 3 SEQUENCE OF PHASES FORMED IN THE REACTED ZONE.

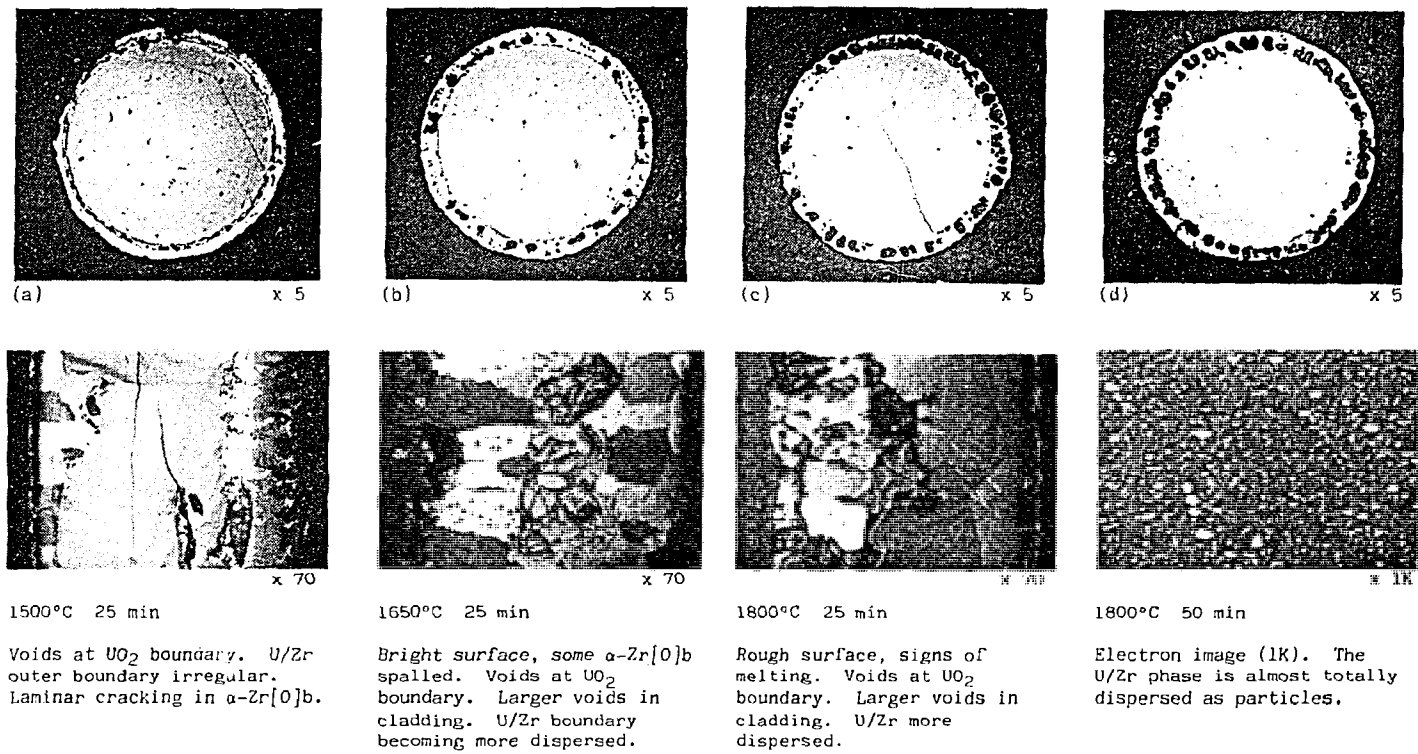
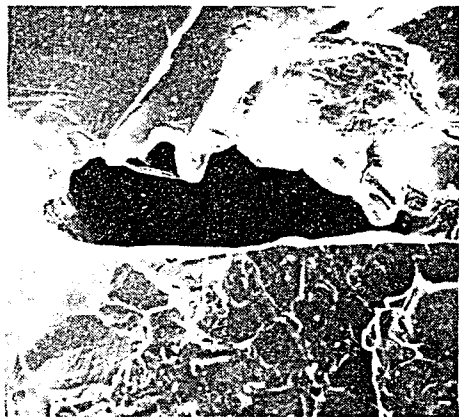


FIG. 4 MICROSTRUCTURES OF FUEL RODS HEATED IN VACUUM AT TEMPERATURES OF 1500, 1650 AND 1800°C.

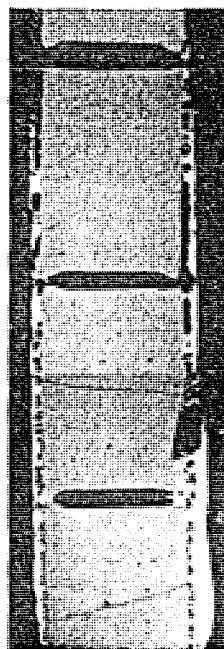


(a) x 50



(b) x 500

FIG. 5 SEM MICROGRAPHS SHOWING FRACTURE SURFACE OF FUEL ROD HEATED TO 1650°C FOR 25 MIN.



x 4



x 100

FIG. 6 MICROSTRUCTURE OF A FUEL ROD HEATED IN VACUUM THROUGH A TEMPERATURE RAMP TO 1850°C.

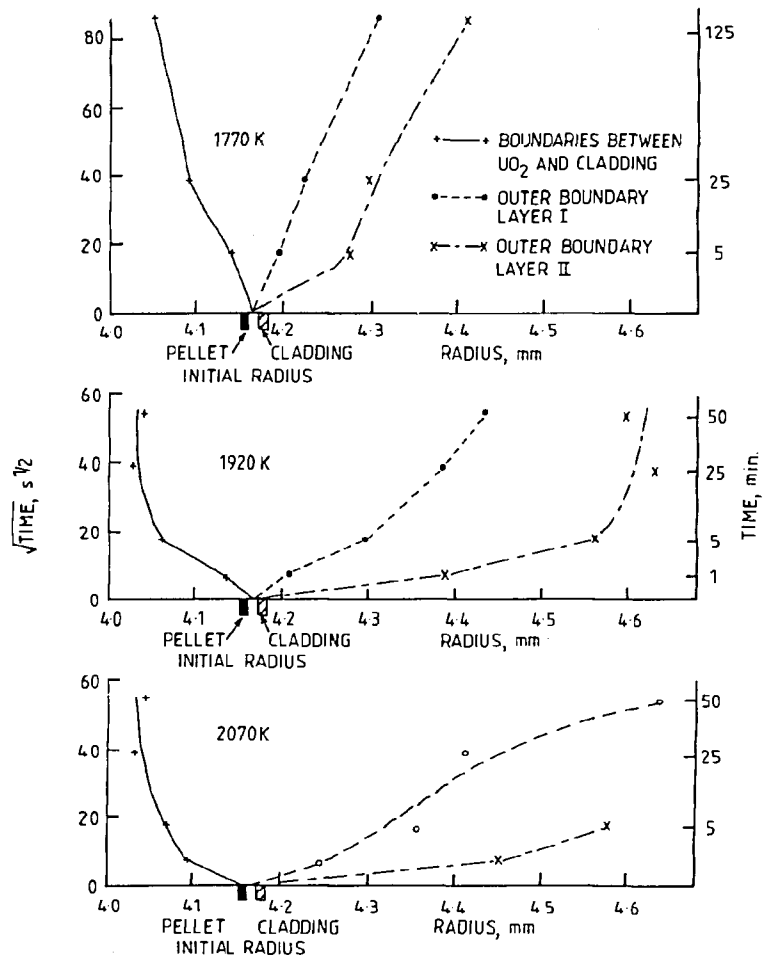


FIG. 7. CHANGE OF LAYER BOUNDARY RADIUS WITH TIME



x 150

FIG. 8 FUEL ROD HEATED TO 1650°C FOR 15 MIN SHOWING POSITION OF TUNGSTEN MARKER WIRE IN $\alpha\text{-Zr(O)}_2$.

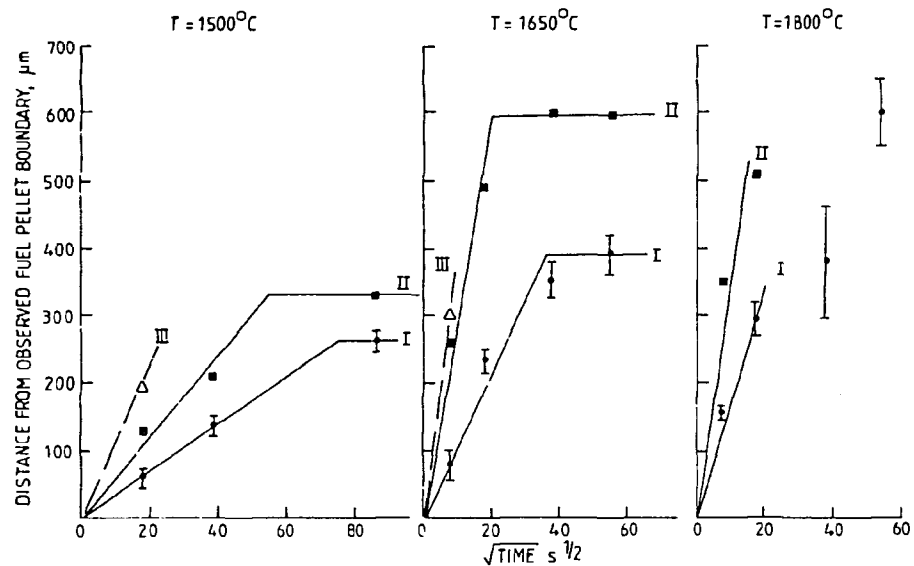


FIG. 9 RATES OF GROWTH OF LAYERS OF REACTION PRODUCTS

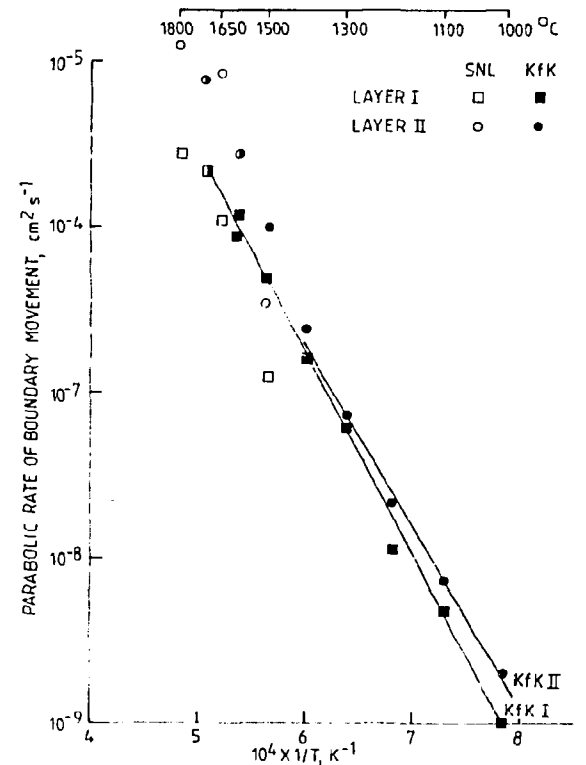


FIG. 10. RATE OF BOUNDARY MOVEMENT VS $1/T$ K^{-1}

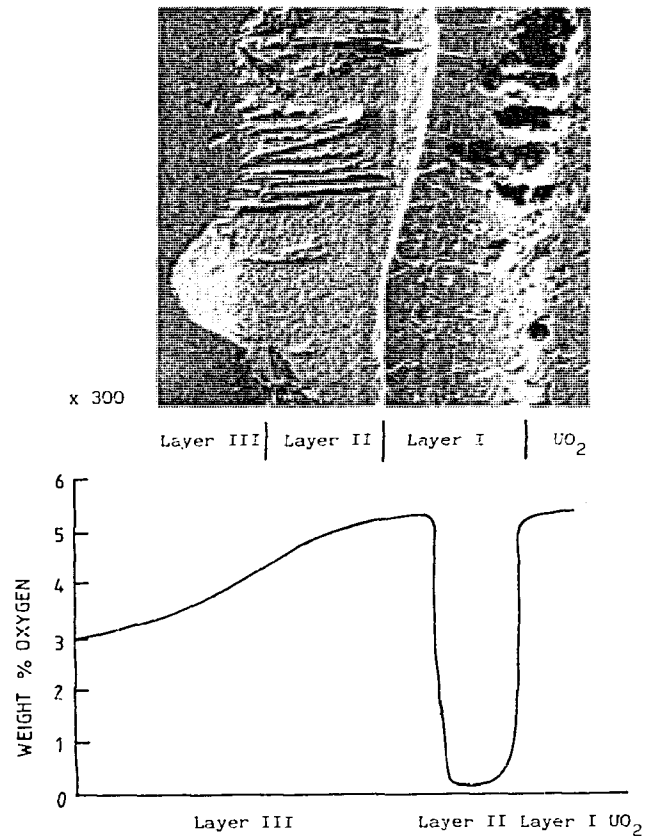


FIG. 11 ELECTRON IMAGE OF UO_2 /ZIRCALOY REACTION ZONE AND OXYGEN DISTRIBUTION IN A FUEL ROD HEATED TO $1500^\circ C$ FOR 5 MIN.

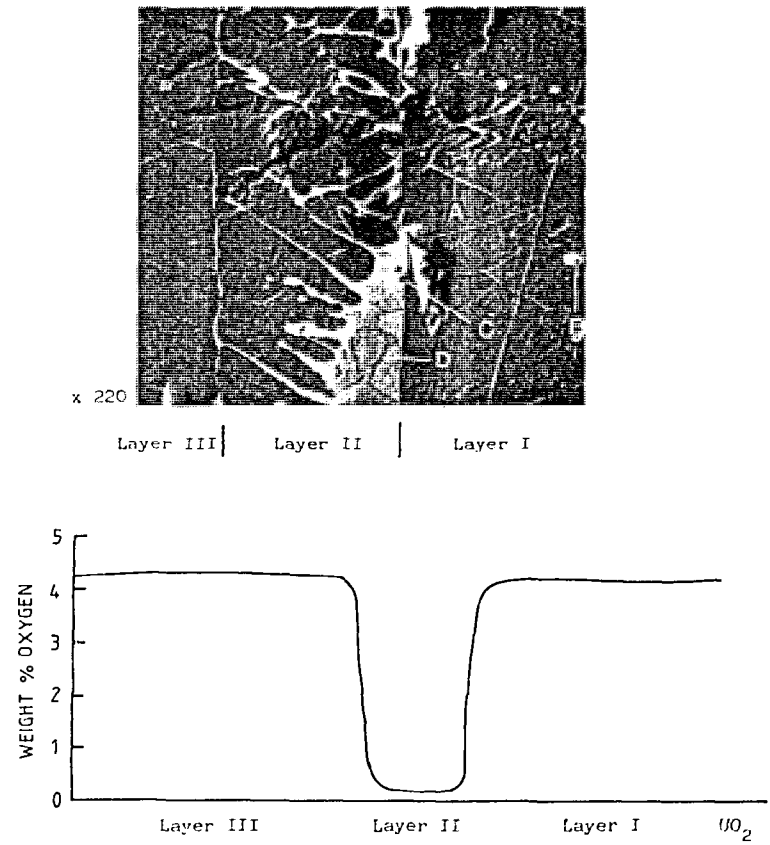


FIG. 12 ELECTRON IMAGE OF THE U/Zr ZONE AND OXYGEN DISTRIBUTION IN A FUEL ROD HEATED AT $1500^\circ C$ FOR 120 MIN.

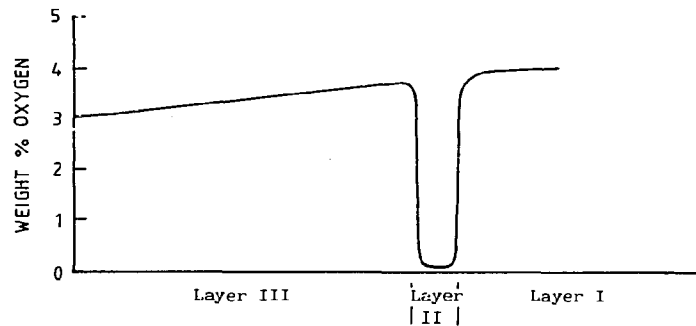
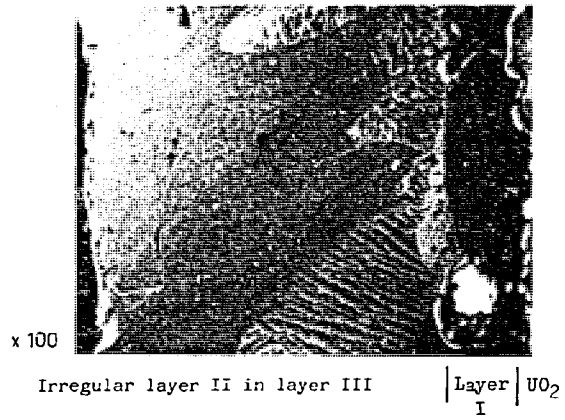


FIG. 13 ELECTRON IMAGE AND OXYGEN DISTRIBUTION FOR FUEL ROD HEATED AT 1800°C FOR 1 MIN.

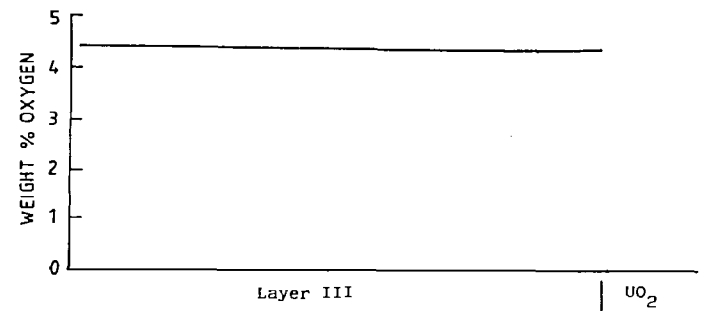
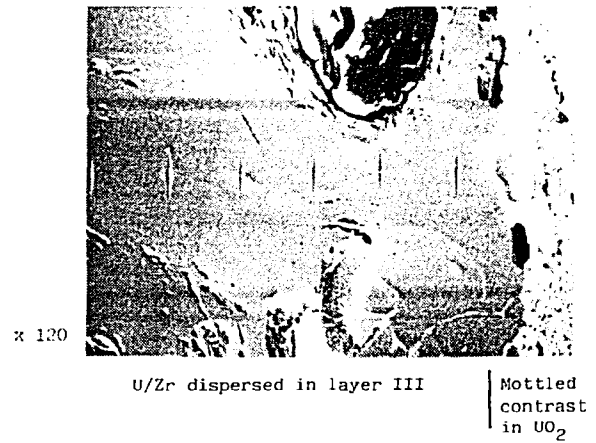


FIG. 14 ELECTRON IMAGE AND OXYGEN DISTRIBUTION FOR FUEL ROD HEATED TO 1800°C FOR 50 MIN.